

Growth of millimeter-sized high-quality CuFeSe₂ single crystals by the molten salt method and study of their semiconducting behavior

Mingwei Ma^{a,c,*}, Binbin Ruan^a, Menghu Zhou^a, Yadong Gu^a, Qingxin Dong^{a,b}, Qingsong Yang^{a,b}, Qiaoyu Wang^{a,d}, Lewei Chen^{a,b}, Yunqing Shi^{a,b}, Junkun Yi^{a,b}, Genfu Chen^{a,b}, Zhian Ren^{a,b}

^a Beijing National Laboratory for Condensed Matter Physics, Institute of Physics, Chinese Academy of Sciences, Beijing 100190, China

^b University of Chinese Academy of Sciences, Beijing 100049, China

^c Songshan Lake Materials Laboratory, Dongguan, Guangdong 100049, China

^d Center for Advanced Quantum Studies and Department of Physics, Beijing Normal University, Beijing 100875, China

ARTICLE INFO

Communicated by Keshra Sangwal

Keywords:

- A1. Supersaturated solutions
- A1. X-ray diffraction
- A2. Growth from solutions
- A2. Single crystal growth
- A3. Molten salt method
- B2. Semiconducting ternary compounds

ABSTRACT

An eutectic AlCl₃/KCl molten salt method in a horizontal configuration was employed to grow millimeter-sized and composition homogeneous CuFeSe₂ single crystals due to the continuous growth process in a temperature gradient induced solution convection. The typical as-grown CuFeSe₂ single crystals in cubic forms are nearly 1.6 × 1.2 × 1.0 mm³ in size. The chemical composition and homogeneity of the crystals was examined by both inductively coupled plasma atomic emission spectroscopy and energy dispersive spectrometer with Cu:Fe:Se = 0.96:1.00:1.99 consistent with the stoichiometric composition of CuFeSe₂. The magnetic measurements suggest a ferrimagnetic or weak ferromagnetic transition below T_C = 146 K and the resistivity reveals a semiconducting behavior and an abrupt increase below T_C.

1. Introduction

Recently, CuFeSe₂ has drawn considerable attention due to its promising applications in thermoelectric technology [1–4], cancer phototherapy [5–8], energy storage systems [9], optoelectronics and solar energy conversion [10–13] as well as their natural abundance, low cost, environmentally friendly nature. It crystallizes in a tetragonal phase with space group $P\bar{4}2c$ and lattice parameters $a = b = 5.53 \text{ \AA}$ and $c = 11.049 \text{ \AA}$, which is a superstructure based upon a cubic close-packed array of anions with the cations occupying a fraction of the available tetrahedral sites as shown in Fig. 1(a) [14]. There are still some controversies about the physical properties of CuFeSe₂. Bulk eskebornite CuFeSe₂ presents a metallic character and a magnetically ordered phase below T_C = 70 K [15–18] whereas several reports on CuFeSe₂ film and nanocrystals reveal a semiconducting behavior [2,19]. Mössbauer absorption measurements indicate a ground state of spin-density waves (SDW) nature in CuFeSe₂ [20] whereas powder neutron scattering and hysteresis loop demonstrate a weak ferrimagnetic behavior [10,18,21,22]. A recent first-principle study reveals that CuFeSe₂ is a direct bandgap semiconductors with forbidden band widths of 0.64 eV

[23] compared with a narrower bandgap of 0.45 eV in CuFeSe₂ nanoparticles [11]. The difference of the physical properties is probably ascribed to various sample defects or grain boundary effects. The single crystal of high quality is the prerequisite for studying the intrinsic physical properties of CuFeSe₂ single crystal which is not reported up to now.

There are several attempts on the crystal growth of CuFeSe₂. The phase transition in solid state of CuFeSe₂ occurs at 570 °C followed by a peritectic dissociation temperature 630 °C and a full melting point at 670 °C [24], implying the incongruent melting of tetragonal CuFeSe₂. Incongruent melting is a process occurring at temperature at which one solid phase transforms to another solid phase and a liquid phase with different chemical compositions than the original composition. CuFeSe₂ crystal was first grown by direct fusion of the elements in stoichiometric proportions or powder sample in a sealed evacuated quartz ampoule heated above its peritectic dissociation temperature [14,24], which will inevitably produce the dissociated phase inside CuFeSe₂ crystals, which is a higher temperature phase of CuFeSe₂ with spinel-type pseudocubic lattice phase [24]. The optimal temperature of crystal growth has to be below the phase transition temperature 570 °C such that a low

* Corresponding author.

E-mail address: mw_ma@iphy.ac.cn (M. Ma).

<https://doi.org/10.1016/j.jcrysgro.2023.127398>

Received 2 July 2023; Received in revised form 10 August 2023; Accepted 11 August 2023

Available online 12 August 2023

0022-0248/© 2023 Elsevier B.V. All rights reserved.

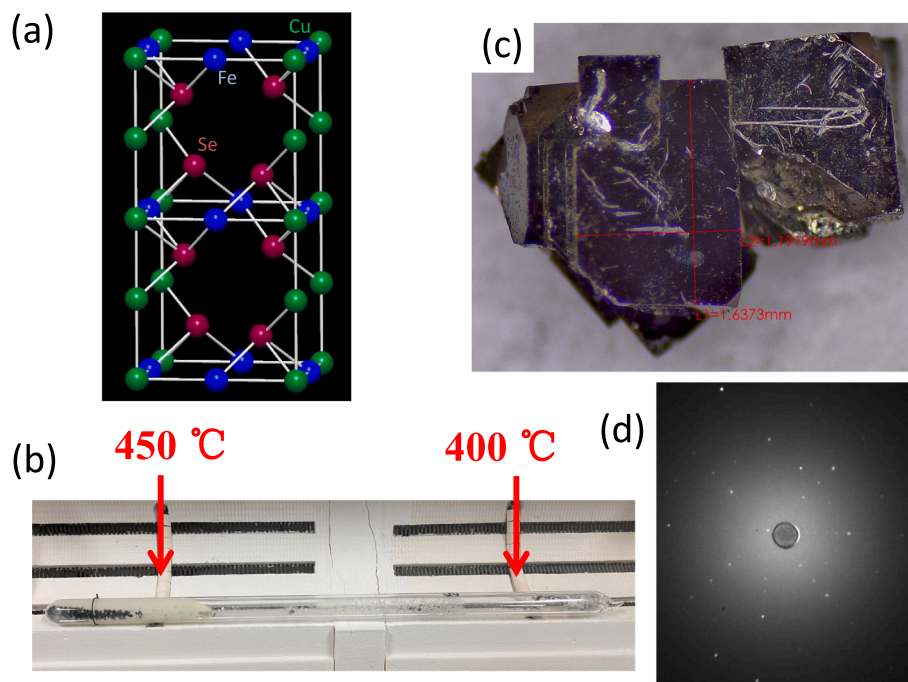


Fig. 1. (a) Crystal structure of CuFeSe_2 . (b) Experimental schemes of the horizontal configuration for a convective AlCl_3/KCl molten salt method by which millimeter-sized CuFeSe_2 single crystals have been grown. (c) Photograph of typical CuFeSe_2 single crystals with cubic shapes and dimensions about $1.6 \times 1.2 \times 1.0 \text{ mm}^3$ grown in present work. (d) Laue picture of CuFeSe_2 single crystal.

temperature growth method with flux or transport agent is indispensable for the perfect single crystal. Single crystals of CuFeSe_2 grown by the gas transport reaction method with I_2 as a transporting agent are 0.7–0.8 cm in size accompanied by intermediate substances FeSeI and $\text{Cu}_3(\text{SeI})_x$ with comparable crystal sizes ($0.8 \times 0.4 \times 0.005 \text{ mm}^3$) [24]. However, they are crystallized in tetragonal lattice with larger parameters $a = b =$

5.91 \AA and $c = 11.82 \text{ \AA}$ and space group of symmetry $I4_2d$ different from the space group $P\bar{4}2c$ of eskebornite CuFeSe_2 . So, another key to a perfect crystal growth is the selection of flux or transport agent which does not react with the raw materials Fe, Cu or Se. AlCl_3/KCl molten salt is a good choice as its melting point is $120 \text{ }^\circ\text{C}$ and no other intermediate

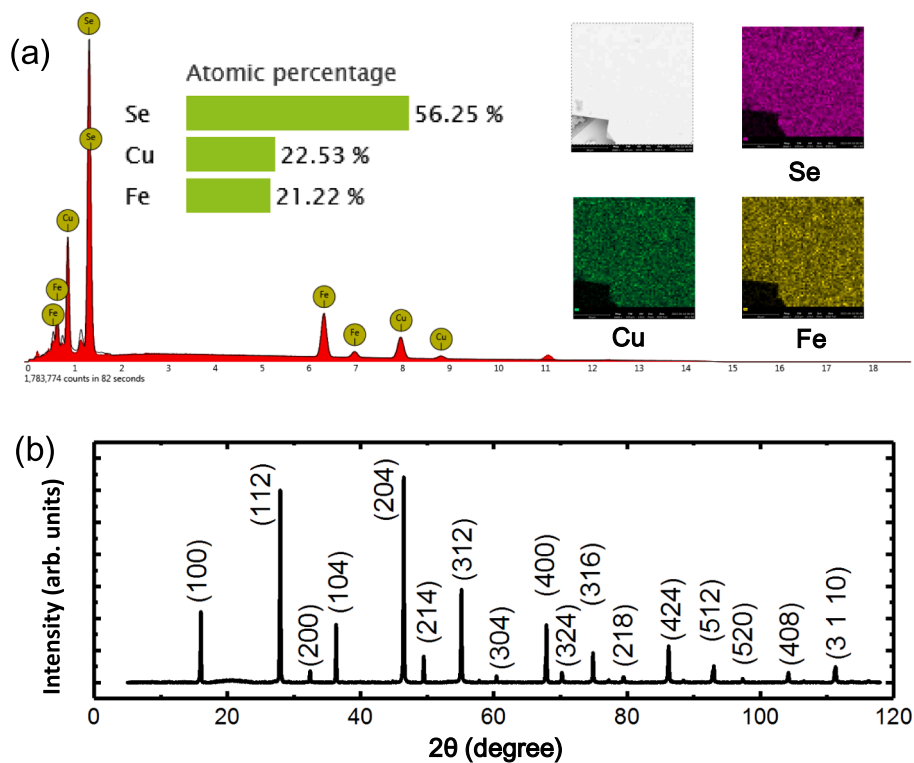


Fig. 2. (a) The EDS microanalysis spectrum taken on the surface area of CuFeSe_2 single crystal. The inset shows the SEM image taken from the flat surface of CuFeSe_2 single crystal and elements Se, Fe, Cu distribution over the surface of CuFeSe_2 single crystal. (b) Powder x-ray diffraction patterns of CuFeSe_2 .

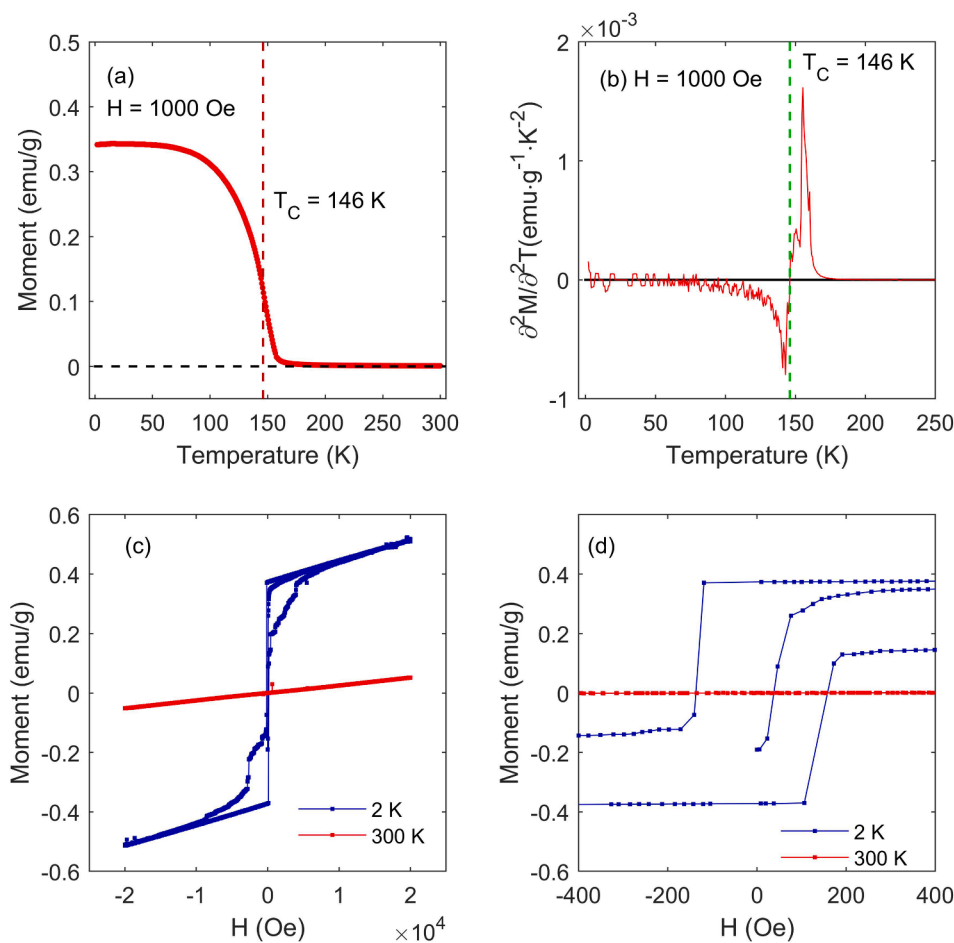


Fig. 3. (a) Temperature dependence of magnetization of CuFeSe₂. (b) The derivative of magnetization $\partial^2 M / \partial^2 T$ versus temperature. (c) Hysteresis loop at 2 K and 300 K. (d) An enlarged view of the hysteresis loop around $H = \pm 400$ Oe.

substances are produced when Fe, Cu or Se dissolved in AlCl₃/KCl solution. In this article we report an eutectic AlCl₃/KCl molten salt method to grow millimeter-sized and composition homogeneous CuFeSe₂ single crystals. The typical as-grown CuFeSe₂ single crystal was nearly $1.6 \times 1.2 \times 1.0$ mm³ in size. In contrast to the previous magnetic and resistivity studies [15–18], our CuFeSe₂ single crystals reveal a semi-conducting behavior and a ferrimagnetic or weak ferromagnetic transition below $T_C = 146$ K.

2. Experimental methods

The raw materials of Fe, Se and Cu powder with molar ratio Fe:Cu:Se = 1:1:2 are mixed together with the salts AlCl₃:KCl = 2:1 in molar ratio and sealed in an evacuated quartz tube ($\phi 10$ mm \times 300 mm). The quartz tube was placed in a horizontal double zone furnace with temperature 450 °C and 400 °C, respectively, resulting in a stable temperature gradient 2 °C/cm as displayed in Fig. 1(b). After a growth duration of 30 days, a large number of high-quality and composition homogeneous CuFeSe₂ single crystals with cubic forms appeared around the cold part of quartz tube. The CuFeSe₂ single crystals are extracted by dissolving the AlCl₃/KCl solvent in distilled water. The typical crystal sizes are up to $1.6 \times 1.2 \times 1.0$ mm³ with regular and flat surfaces as shown in Fig. 1(c). Fig. 1(d) shows an example of back-scattering x-ray Laue patterns obtained on (001) plane (*ab* plane) of CuFeSe₂ single crystal. The result shows very sharp and uniform diffraction spots with the 4-fold axis symmetry demonstrating the crystalline perfection of the CuFeSe₂ single crystal without twin crystals.

It should be emphasized that conventional flux growth is usually

carried out in a vertical configuration of the furnace. The single crystals are grown by slow cooling the supersaturated solution. In our case, CuFeSe₂ has low solubility in AlCl₃/KCl solution due to the limitation of the lower growth temperature. Also, the narrower temperature range for crystallization is the obstacle to a continuous growth process of CuFeSe₂ single crystals. The horizontal configuration with stable temperature gradient can effectively overcome or compensate the above limitations at the expense of longer growth duration of 30 days.

The micro-morphology of CuFeSe₂ single crystals was examined by scanning electron microscope (SEM) on Phenom ProX. The chemical composition was determined by both inductively coupled plasma atomic emission spectroscopy (ICP) and energy dispersive spectrometer (EDS) on Phenom ProX. Powder x-ray diffraction measurements were carried out at room temperature on an x-ray diffractometer (Rigaku UltimaIV) using Cu K_α radiation. The resistance of crystal sample was measured on Quantum Design PPMS-9 using the standard 4-probe method. The magnetic measurements were carried out on a SQUID magnetometer (Quantum Design MPMS XL-1).

3. Results and discussion

The chemical composition and homogeneity of the crystals was examined by the EDS analysis and one of the typical EDS spectrums taken on the crystal surface is shown in Fig. 2(a). The composition of the crystal is very homogeneous as demonstrated in the insets of Fig. 2(a). The mapping areas with purple, green and yellow represent the homogeneous distribution of Se, Cu and Fe, respectively. The chemical composition is roughly estimated to be Cu:Fe:Se = 22.53:21.22:56.25 ≈

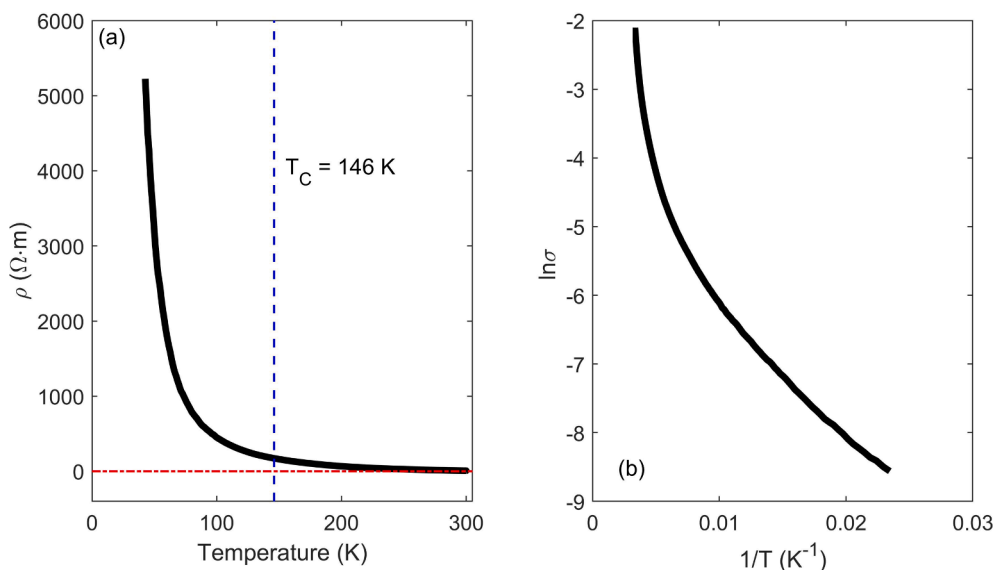


Fig. 4. (a) Temperature dependence of resistivity of CuFeSe₂. (b) Temperature dependence of conductivity ($\ln\sigma$ vs $1/T$) of CuFeSe₂.

0.90:0.85:2.25. The deviation of stoichiometry of Cu:Fe:Se = 1:1:2 is probably attributed to the measurement only on the surface of crystals. For a more accurate determination of the chemical composition, several crystals are ground into powder measured by ICP, which gives the molar ratio with Cu:Fe:Se = 0.96:1.00:1.99, which is consistent with the stoichiometric composition of CuFeSe₂. Fig. 2(b) shows the powder x-ray diffraction (XRD) patterns of CuFeSe₂ at room temperature. Powder XRD demonstrates that all the diffraction peaks of CuFeSe₂ can be well indexed with a previously reported tetragonal structure with the space group of $P\bar{4}2c$ and lattice parameters $a = 5.5190(3)$ Å and $c = 11.0488(7)$ Å. No impurity peaks can be observed in our XRD spectrum indicating the high purity and quality of our CuFeSe₂ single crystals.

As we know, the grain boundary in powder sample and impurity intergrown with CuFeSe₂ will conceal its intrinsic properties. After characterization of the high purity and quality of CuFeSe₂ single crystal, we turn to its magnetic and electrical properties. Fig. 3(a) shows the temperature dependence of magnetic susceptibility ranging from 2 K to 300 K which displays a paramagnetic and ferrimagnetic behaviour above and below T_C respectively. Fig. 3(b) shows the derivative of magnetization $\partial^2 M / \partial^2 T$ versus temperature which suggest the $T_C \approx 146$ K. Previous reports on CuFeSe₂ sample showed paramagnetic behavior from room temperature down to $T_C \approx 70$ K or 80 K, below which the Fe atoms on the $2e$ and $2a$ sites (of the tetragonal cell) have slightly different magnetic moments, resulting in a weak ferrimagnetic behavior [15–18]. To verify the magnetic response of the CuFeSe₂ single crystals, the hysteresis loops were measured at 2 and 300 K and between $-20,000$ Oe and $+20,000$ Oe and the results are presented in Fig. 3(c). The hysteresis loop suggests a ferrimagnetic behaviour at 2 K and a paramagnetic behaviour at 300 K. At both temperatures, the hysteresis loop has a slanted appearance which is not saturated at 20,000 Oe, consistent with previous measurements on CuFeSe₂ nanocrystals [10,25]. The enlarged view between $H = \pm 400$ Oe is displayed in Fig. 3(d), where the coercive force $H_c \approx 130$ Oe at $T = 2$ K in contrast to 1360 Oe or 1780 Oe on CuFeSe₂ nanocrystals [10,22]. Also, there still exist non-linear S-shape curve in hysteresis loop at room temperature in previous report indicating possible ferromagnetic impurity in their samples [10,22,25]. The linear behavior in our hysteresis loop at 300 K suggests the high purity of our as-grown CuFeSe₂ single crystals. Fig. 4 (a-b) shows the temperature dependence of resistivity and conductivity which reveals a semiconducting behavior in agreement with the results on CuFeSe₂ thin films or nanocrystals [2,19] instead of a metallic character in CuFeSe₂ bulk sample [15]. The differences in magnetic and

electrical properties on various CuFeSe₂ samples synthesized via different preparation process is probably due to size effects, surface effects, interparticle interactions or impurities inside the previous sample.

4. Conclusion

We have grown millimeter-sized CuFeSe₂ single crystals using eutectic AlCl₃/KCl molten salt in a quartz ampoule placed in a double temperature zone furnace of horizontal configuration. The clear Laue spots and linear behavior of the hysteresis loops at 300 K indicates the high quality of CuFeSe₂ single crystals without any other magnetic impurities. A ferrimagnetic or weak ferromagnetic transition was observed below $T_C = 146$ K where the resistivity shows an abrupt enhancement which reflect the intrinsic properties of CuFeSe₂ single crystals.

CRediT authorship contribution statement

Mingwei Ma: Conceptualization, Methodology, Writing – review & editing. **Binbin Ruan:** Software. **Menghu Zhou:** Software. **Yadong Gu:** Software. **Qingxin Dong:** Software. **Qingsong Yang:** Software. **Qiaoyu Wang:** Software. **Lewei Chen:** Software. **Yunqing Shi:** Software. **Junkun Yi:** Software. **Genfu Chen:** Conceptualization, Methodology. **Zhian Ren:** Conceptualization, Methodology.

Declaration of Competing Interest

The authors declare that they have no known competing financial interests or personal relationships that could have appeared to influence the work reported in this paper.

Data availability

Data will be made available on request.

Acknowledgments

We gratefully thank Lihong Yang, Hongjun Shi, Li Wang and Youting Song for their technical help in x-ray diffraction and chemical analysis. The work was supported by the National Natural Science Foundation of China (Grant No. 12004418), the National Key Research and Development of China (Grant No. 2018YFA0704200, 2022YFA1602800) and the Strategic Priority Research Program of Chinese Academy of Sciences

(Grant No. XDB25000000).

References

- [1] M. Moorthy, A. Bhui, M. Battabyal, S. Perumal, Nanostructured CuFeSe₂ Eskebornite: an efficient thermoelectric material with ultra-low thermal conductivity, *Mater. Sci. Eng. B* 284 (2022), 115914, <https://doi.org/10.1016/j.mseb.2022.115914>.
- [2] J. Zhai, H. Wang, W. Su, T. Wang, F. Mehmood, X. Wang, T. Chen, T. Huo, K. Zhang, C. Wang, The p-n transformation and thermoelectric property optimization of Cu_{1+x}FeSe₂ (x = 0–0.05) alloys, *J. Mater. Chem. C* 7 (2019) 9641–9647, <https://doi.org/10.1039/C9TC01607D>.
- [3] P.C. Lee, M.N. Ou, J.Y. Luo, M.K. Wu, Y.Y. Chen, Cross-plane Seebeck coefficient and thermal conductivity of CuFeSe₂ thin film, *AIP Conf. Proc.* 1449 (1) (2012) 405–408, <https://doi.org/10.1063/1.4731582>.
- [4] B.-Q. Zhang, Y. Liu, Y. Zuo, J.-S. Chen, J.-M. Song, H.-L. Niu, C.-J. Mao, Colloidal synthesis and thermoelectric properties of CuFeSe₂ nanocrystals, *Nanomaterials* 8 (1) (2018) 8, <https://doi.org/10.3390/nano8010008>.
- [5] M. Liu, D. R. Radu, G. S. Selopal, S. Bachu, C.-Y. Lai, Stand-Alone CuFeSe₂ (Eskebornite) nanosheets for photothermal cancer therapy, *Nanomaterials* 11(8) (2021) 2008, <https://doi.org/10.3390/nano11082008>.
- [6] X. Jiang, S. Zhang, F. Ren, L. Chen, J. Zeng, M. Zhu, Z. Cheng, M. Gao, Z. Li, Ultrasmall magnetic CuFeSe₂ ternary nanocrystals for multimodal imaging guided photothermal therapy of cancer, *ACS Nano* 11 (6) (2017) 5633–5645, <https://doi.org/10.1021/acsnano.7b01032>.
- [7] L.-Y. Lai, Y. Jiang, G.-P. Su, M. Wu, X.-F. Lu, S.-Z. Fu, L. Yang, J. Shu, Gadolinium-chelate functionalized magnetic CuFeSe₂ ternary nanocrystals for T1–T2 dual MRI and CT imaging in vitro and in vivo, *Mater. Res. Exp.* 8 (2021), 045001, <https://doi.org/10.1088/2053-1591/abf1a2>.
- [8] W. Dang, T. Li, B. Li, H. Ma, D. Zhai, X. Wang, J. Chang, Y. Xiao, J. Wang, C. Wu, A bifunctional scaffold with CuFeSe₂ nanocrystals for tumor therapy and bone reconstruction, *Biomaterials* 160 (2018) 92–106, <https://doi.org/10.1016/j.biomaterials.2017.11.020>.
- [9] P. Anjana, P.R. Ranjani, R. Rakhi, Cu-Fe based oxides and selenides as advanced electrode materials for high performance symmetric supercapacitors, *Mater. Lett.* 296 (2021), 129827, <https://doi.org/10.1016/j.matlet.2021.129827>.
- [10] W. Wang, J. Jiang, T. Ding, C. Wang, J. Zuo, Q. Yang, Alternative synthesis of CuFeSe₂ nanocrystals with magnetic and photoelectric properties, *ACS Appl. Mater. Interfaces* 7 (4) (2015) 2235–2241, <https://doi.org/10.1021/am508844w>.
- [11] H. Liu, C. Chen, H. Wen, R. Guo, N.A. Williams, B. Wang, F. Chen, L. Hu, Narrow bandgap semiconductor decorated wood membrane for high-efficiency solar-assisted water purification, *J. Mater. Chem. A* 6 (2018) 18839–18846, <https://doi.org/10.1039/C8TA05924A>.
- [12] P. Kowalik, P. Bujak, M. Penkala, K. Kotwica, A. Kmita, M. Gajewska, A. Ostrowski, A. Pron, Synthesis of CuFeSe_{2-x}Se_x – alloyed nanocrystals with localized surface plasmon resonance in the visible spectral range, *J. Mater. Chem. C* 7 (2019) 6246–6250, <https://doi.org/10.1039/C9TC01242G>.
- [13] A. Sun, X. Hou, X. Hu, Super-performance photothermal conversion of 3D macrostructure graphene-CuFeSe₂ aerogel contributes to durable and fast clean-up of highly viscous crude oil in seawater, *Nano Energy* 70 (2020), 104511, <https://doi.org/10.1016/j.nanoen.2020.104511>.
- [14] J. Delgado, G. de Delgado, M. Quintero, J. Woolley, The crystal structure of copper iron selenide, CuFeSe₂, *Mater. Res. Bull.* 27 (3) (1992) 367–373, [https://doi.org/10.1016/0025-5408\(92\)90066-9](https://doi.org/10.1016/0025-5408(92)90066-9).
- [15] J. Lamazares, F. Gonzalez-Jimenez, E. Jaimes, L. D'Onofrio, R. Iraldi, G. Sanchez-Porras, M. Quintero, J. Gonzalez, J. Woolley, G. Lamarche, Magnetic, transport, X-ray diffraction and Mössbauer measurements on CuFeSe₂, *J. Magn. Magn. Mater.* 104–107 (1992) 997–998, [https://doi.org/10.1016/0304-8853\(92\)90459-2](https://doi.org/10.1016/0304-8853(92)90459-2).
- [16] A.M. Polubotko, Ferron-type conductivity in metallic CuFeSe₂, *Phys. Met. Metallogr.* 112 (2011) 589–590, <https://doi.org/10.1134/S0031918X11060093>.
- [17] J. Lamazares, E. Jaimes, L. D'Onofrio, F. Gonzalez-Jimenez, G. Sanchez Porras, R. Tovar, M. Quintero, J. Gonzalez, J.C. Woolley, G. Lamarche, Magnetic susceptibility, transport and Mössbauer measurements in CuFeSe₂, *Hyperfine Interact* 67 (1991) 517–521, <https://doi.org/10.1007/BF02398194>.
- [18] J. Woolley, A.-M. Lamarche, G. Lamarche, R. Brun del Re, M. Quintero, F. Gonzalez-Jimenez, I. Swainson, T. Holden, Low temperature magnetic behaviour of CuFeSe₂ from neutron diffraction data, *J. Magn. Magn. Mater.* 164 (1) (1996) 154–162, [https://doi.org/10.1016/S0304-8853\(96\)00365-4](https://doi.org/10.1016/S0304-8853(96)00365-4).
- [19] N. Hamdadou, M. Morsli, A. Khelil, J.C. Bernede, Fabrication of n- and p-type doped CuFeSe₂ thin films achieved by selenization of metal precursors, *J. Phys. D: Appl. Phys.* 39 (2006) 1042, <https://doi.org/10.1088/0022-3727/39/6/008>.
- [20] F. Gonzalez-Jimenez, E. Jaimes, A. Rivas, L. D'Onofrio, J. Gonzalez, M. Quintero, New spin-density waves systems: Cu and Fe selenides and tellurides, *Physica B* 259–261 (1999) 987–989, [https://doi.org/10.1016/S0921-4526\(98\)00930-2](https://doi.org/10.1016/S0921-4526(98)00930-2).
- [21] T. Yang, M. Fang, J. Liu, D. Yang, Y. Liang, J. Zhong, Y.-J. Yuan, Y. Zhang, X. Liu, R. Zheng, K. Davey, J. Zhang, Z. Guo, Ultranarrow bandgap Se-deficient bimetallic selenides for high performance alkali metal-ion batteries, *Adv. Funct. Mater.* 32 (2022) 22058, <https://doi.org/10.1002/adfm.202205880>.
- [22] E. Dutkova, I. Skorvanek, M.J. Sayagues, A. Zorkovska, J. Kovac, P. Balaz, Mechanochemically synthesized cufese₂ nanoparticles and their properties, *Acta Phys. Polon. A* 131 (2017) 1156–1158, <https://doi.org/10.12693/APhysPolA.131.1156>.
- [23] X. Liu, J. Du, L. Hua, K. Liu, First-principles comparative study of CuFeSe₂ and CuFeS₂, *Mater. Res.* 26 (2023) e20220371.
- [24] A. Najafov, G. Guseinov, O. Alekperov, Growth technology and X-ray investigation results of CuFeSe₂ crystal modifications, *J. Phys. Chem. Solid* 64 (9) (2003) 1873–1875, [https://doi.org/10.1016/S0022-3697\(03\)00200-2](https://doi.org/10.1016/S0022-3697(03)00200-2).
- [25] N. Wu, Y. Li, M. Zeng, J. Gao, Y. Tang, Z. Zeng, Y. Zheng, Design of chalcopyrite-type CuFeSe₂ nanocrystals: microstructure, magnetism, photoluminescence and sensing performances, *J. Solid State Chem.* 271 (2019) 292–297, <https://doi.org/10.1016/j.jssc.2019.01.015>.